Constraints on the exhumation and erosion of the High Himalayan Slab, NW India, from foreland basin deposits

Nikki M. White [a],*, M. Pringle [b], E. Garzanti [c], M. Bickle [a], Y. Najman [d], H. Chapman [a], P. Friend [a]

[a] *Department of Earth Sciences, Downing Street, Cambridge CB2 3EQ, UK*
[b] *Scottish Universities Environmental Research Centre, Scottish Enterprise Technology Park, Rankine Avenue, East Kilbride, Scotland, UK*
[c] *Dipartimento di Scienze Geologiche e Geotecnologie, Piazza della Scienza 4, 20126 Milan, Italy*
[d] *Department of Geology and Geophysics, University of Edinburgh, Grant Institute, West Mains Road, Edinburgh EH9 3JW, Scotland, UK*

Abstract

Petrography, Sr–Nd isotope compositions and single-grain laser ^{40}Ar–^{39}Ar ages of detrital white mica from Early–Middle Miocene molasse of the Dharamsala and Lower Siwalik Formations of Northern India, dated by magnetostratigraphy, determine the sediment sources, their metamorphic grade and exhumation rates in the Himalayan palaeo-hinterland. Deposition of the Lower Dharamsala Member (21–17 Ma) occurred during the period of rapid isothermal decompression and crustal anatexis (24–18 Ma) of the metamorphic core. This episode of decompression is thought to be coeval with thrusting on the Main Central Thrust and normal faulting on the South Tibetan Detachment System. The sediment composition and detrital mica ages indicate erosion from the rapidly exhumed metamorphic slab of the High Himalayan Crystalline Series. Deposition of the Upper Dharamsala Member (17–13 Ma) and basal Siwalik Group (13–12.5 Ma) spanned the period in which thrusting transferred south from the Main Central Thrust. The sediment composition and detrital mica ages contrast strongly with those of the Lower Dharamsala, indicating erosion from sedimentary and low grade rocks. The isotopic composition indicates that these rocks were part of the High Himalayan Series unaffected by Tertiary metamorphism, i.e. from upper structural levels of the High Himalayan Slab. This suggests that a major reorganisation of the orogenic wedge occurred at 17 Ma involving forward propagation of the MCT and cessation of rapid exhumation of the metamorphic slab. © 2002 Elsevier Science B.V. All rights reserved.

Keywords: Himalayas; exhumation; Siwalik System; provenance

1. Introduction

The mechanisms and rates of crustal thickening and exhumation govern both the topographic evolution and the formation, preservation and outcrop patterns of metamorphic facies in orogen-

---

* Corresponding author. Tel.: +44 (131 650 7010;
Fax: +44 131 668 3184.
  E-mail address: nicola_clarke@onetel.net.uk (N.M. White).

ic belts [1]. However, the processes which control exhumation of thickened crust and the contribution surface processes make to exhumation are controversial [2–4]. For the purpose of unravelling the evolution of an orogenic system, sedimentary basins adjacent to the orogenic belt contain an easily accessible, long term record of the erosional denudation products. These can point to the structural and thermal evolution of the palaeo-hinterland and can provide additional constraint upon orogenic models [2,5].

The Himalaya–Tibet region is a prime example of deformation in a zone of continental collision. Following collision, Eocene and Oligocene thrusting and recumbent folding in the Himalayas led to crustal thickening and metamorphism. This was subsequently exhumed in the Miocene by thrusting on the Main Central Thrust (MCT) and coeval normal faulting high in the section. The surface expression of thrusting subsequently transferred south to the Main Boundary Thrust and the presently active Main Frontal Thrust. Estimates of the timing, duration and displacement of these thrusting episodes are largely based on metamorphic and geochronological data, restricted to the presently exposed rocks. This information is insufficient to answer critical questions concerning the identity and rates of exhumation of major tectonic units and the significance of the major faults in controlling the evolution of the Himalayan orogen.

In this paper, we apply petrography, ^{40}Ar–^{39}Ar total fusion and incremental-heating chronology of single detrital white–micas, and Sr–Nd isotopic mapping of source provenance to a dated section of foreland basin sediments in Himachal Pradesh, NW India deposited between 20.5 and 12.5 Ma [6]. The results constrain the provenance and exhumation history of the hinterland during this time and emphasise the significance of major faults in controlling deformation and exhumation on time scales of tens of millions of years. Comparison of these results with the Bengal Fan sedimentary record demonstrates the importance of studies on catchment-scales of hundreds of km^2, as well as regional scales of hundreds of km^2, in relating sediment provenance to the structural, metamorphic, and exhumation history of the Himalayas.

2. Geology and uplift history

2.1. Geology of the NW Indian Himalayas

The Himalayas result from the collision of the northern margin of the Indian continental plate with Eurasia > 50 Myr ago [7]. The Indian plate rocks include Early Proterozoic to Phanerozoic continental margin sequences (Fig. 1). The Indus–Tsangpo suture zone contains ophiolites and volcaniclastic turbidites and represents the site of the continental collision. South of the Indus–Tsangpo suture zone the Tibetan Sedimentary Series (TSS) comprises a fold and thrust belt of mainly sub-greenschist facies Palaeozoic and Mesozoic Tethyan sediments [8,9]. The TSS are juxtaposed against high grade migmatites, leucogranites, and gneisses of the High Himalayan Crystalline Series (HHCS) [10] along the extensional Zanskar Shear Zone, the NW Indian segment of the South Tibetan Detachment System (STDS) a family of low-angle north dipping normal faults. The HHCS are thrust over the unmetamorphosed or low grade late Palaeoproterozoic (meta) sediments, minor volcanics, and granitic components [11] of the Lesser Himalayan Series (LHS) by the MCT a crustal scale ductile shear zone as seen in the Kulu Window (Fig. 1).

In the NW Indian Himalaya, the protolith rocks of the HHCS are thought to include low grade Proterozoic metagreywackes, metasiltstones and Cambro–Ordovician granitoid gneisses of the Haimantas [12] or Kade Formation [13]. Palaeozoic to Mesozoic Tethyan sediments which include carbonaceous shales, limestones, and dolomitic limestone, unconformably overlie the Haimantas and are preserved south of, and structurally above the HHCS in the Chamba Nappe [12] (Fig. 1). The Chamba Nappe is separated from the HHCS by a syn-metamorphic shear zone the Miyar Thrust [13] or the Chenab Normal fault [12], although it has been argued that the HHCS and overlying Chamba Nappe forms a more-or-less coherent tectonic unit (the High Himalayan Slab) that has experienced a polyphase deformation history [14]. This outcrop pattern is unlike that of the Central Himalaya where low grade HHCS and TSS are not present south of
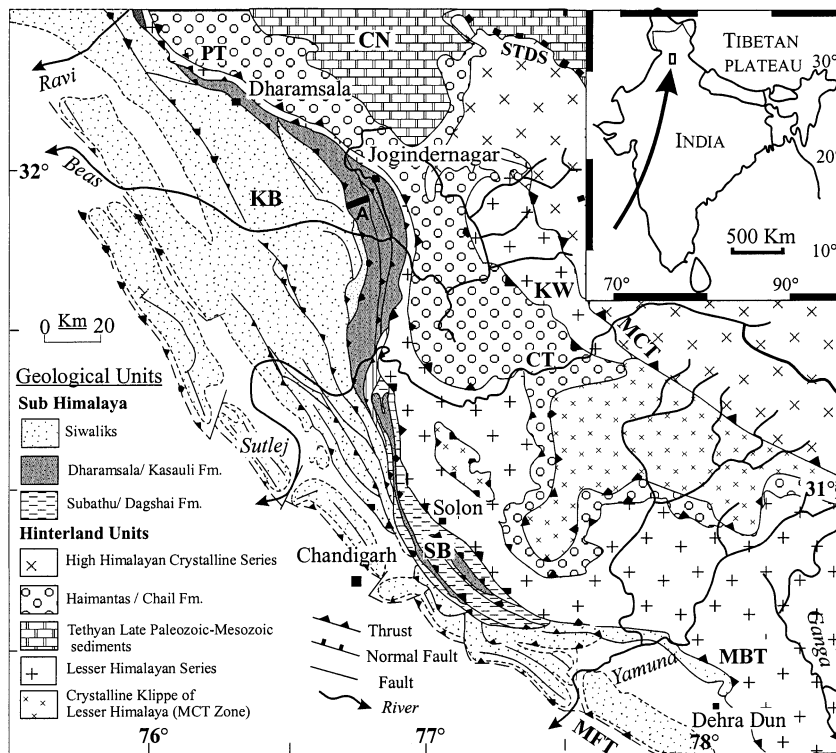
Fig. 1. Geological map of the North Indian Himalaya, boxed inset shows location of map. Section A shows the location of this study. Major Himalayan faults are marked; STDS, South Tibetan Detachment System; MCT, Main Central Thrust; MBT, Main Boundary Thrust; MFT, Main Frontal Thrust. Selected local faults are labelled; PT, Panjal Thrust; CT, Chail Thrust. The Kangra Basin (KB), Subathu Basin (SB), Chamba Nappe (CN), and the Kulu Window (KW) are also labelled. The map is adapted from Powers et al. [15] and Thakur [12].

the HHCS. The isograds in the crystalline units form patterns of metamorphic domes and depressions with no major structural or metamorphic discontinuities between chlorite and sillimanite zones indicating exhumation to deeper and shallower levels within the slab [14]. The MCT, as defined as juxtaposing the HHCS above the LHS, is exposed only in the Kitshtwar and Kulu windows. Further south the MCT is often marked as defining the contact between the low grade and sedimentary units of the Chamba Nappe and the Lesser Himalaya. This thrust is also known as the Panjal Thrust [12]. The LHS is thrust over the Sub-Himalayas, comprising Palaeogene and Neogene units of the foreland basin, by the Main Boundary Thrust and the Sub-Himalaya are emplaced over the youngest units of the foreland basin sediments by the Main Frontal Thrust.

2.2. Structural evolution

The Indo–Asian collision at ∼ 50 Ma caused folding, thrusting and crustal thickening of the northern margin of the Indian plate. This resulted in kyanite grade Barrovian metamorphism of the deeper levels of crust at ∼ 40–25 Ma [16]. Mineral fabrics and compositional zoning which indicate near isothermal decompression into the sillimanite field, fluid-absent partial melting which produced leucogranites with ages mainly between 24 and 12 Ma [17] and mica cooling ages which lie in the period 25–15 Ma [17] demonstrate that the Barrovian metamorphism was terminated by rapid decompression. The cause of decompression has been related to the initiation of extensional faulting along the STDS, active from at least ∼ 22 Ma to 19.8 Ma [14,18] and synchronous movement
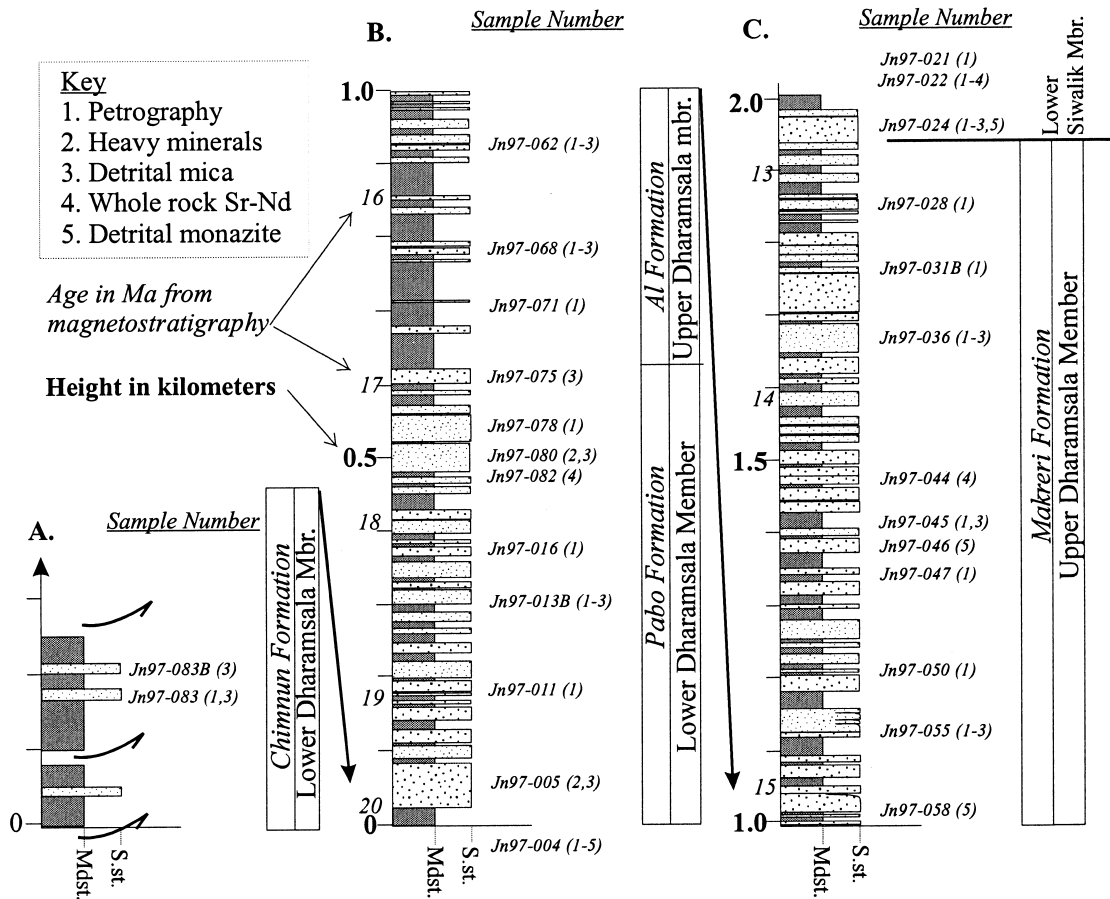
Fig. 2. Dharamsala Group Stratigraphy (Section A, Fig. 1). Position of samples selected for analyses and the types of analyses are shown. Height in km (bold) and age of deposition (italics) as correlated to magnetostratigraphy [6] are shown on the left. Column A is discontinuous and incomplete due to tectonic disruption by thrusting, Columns B and C are continuous and represent largely complete sections.

along the MCT (initiated by ∼23 Ma [19]). The Main Boundary Thrust was initiated by ∼10 Ma [20] and in the present day Himalaya, convergence is largely accommodated along the Main Frontal Thrust [21].

2.3. Foreland basin

Erosion of the Himalayas has produced detritus which is deposited in the Indus and Bengal ocean fans or in the south flanking foreland basin (the Sub-Himalayas). Himalayan foreland basin deposits are exposed by thrusting above the Main Frontal Thrust (Fig. 1). The oldest rocks are Late Palaeocene to Middle Eocene carbonates with a

low clastic input, and mineralogy and Nd–Sr isotopic composition characteristic of Indus–Tsangpo suture zone rocks and Tethyan Sediments [22,23] (annotated on Fig. 8). Late Eocene and early Oligocene rocks are absent. Upper Oligocene, Miocene, and younger rocks are continental fluvial, lacustrine or deltaic sediments. Deposition of the Dharamsala or Murree Group in the Oligocene and Early Miocene was followed by the Middle Miocene to Early Pleistocene fluvial Siwalik Group with depositional ages established by magnetostratigraphy, ash horizons, and mammalian fauna [24].

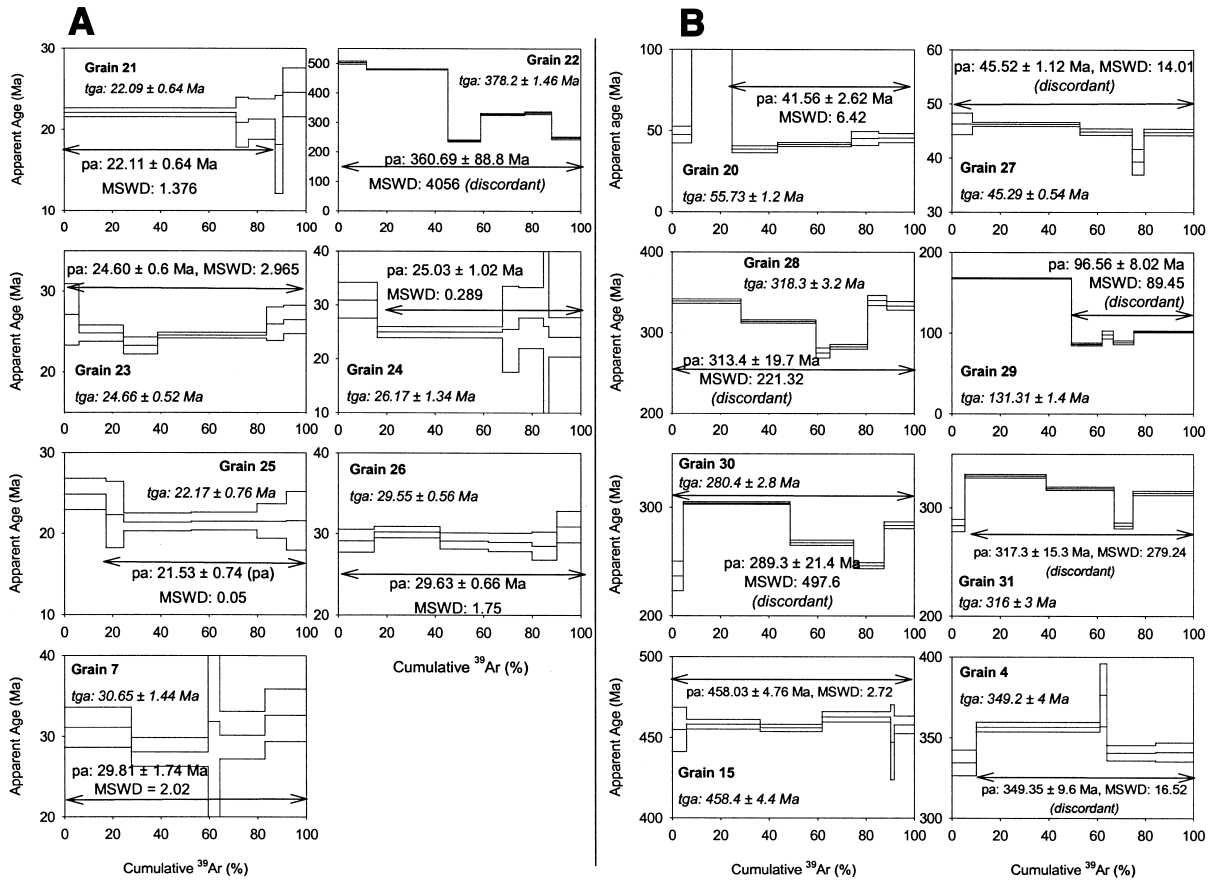This paper focuses on a section of early foreland basin strata of the Dharamsala Group to

Fig. 3. Incremental-heating plots. $^{40}Ar/^{39}Ar$ release spectrum diagrams for single white mica grains from samples JN97-005 (A) and JN97-022 (B). Arrows indicate the increments used for calculating plateau ages. Plateau ages (pa) and total gas ages (t_{ga}) are given for each grain. Errors plotted and quoted are to 2σ.

Lower Siwalik Sub-Group in Himachal Pradesh, NW India (Fig. 1), dated by magnetostratigraphy (Fig. 2) [6]. These crop out in the Kangra basin NW along strike of the Late Oligocene and Miocene Dagshai and Kasauli Formations in the Subathu basin (Fig. 1). The Dharamsala Group comprises an Upper and Lower Member (17–13 and 20–17 Ma respectively). The Lower Member comprises the Chimnun and Pabo Formations and the Upper Member comprises the Al and Makreri Formations (adapted from [25]; Fig. 2). Deposited in a continental setting the multistoried sandstones, which are most prevalent in the Pabo and Makreri Formations, are interpreted as channel deposits of large braided rivers. Finer grained facies of the Chimnun and Al Formations, consisting of thick mudstones and siltstones with interbedded sandstone beds, may represent overbank sediments deposited on adjacent floodplains subjected to periodic inundation by crevasse splay and sheet flows [26].

3. Analytical methods

3.1. $^{40}Ar–^{39}Ar$ detrital white mica analyses

Single grains of white micas (200–350 μm) handpicked from 14 sandstone samples (Fig. 2) were loaded into individual wells in 42 well, 22 mm diameter 99.99+% pure Cu disks. Twelve disks were irradiated for 6 h in the in-core,
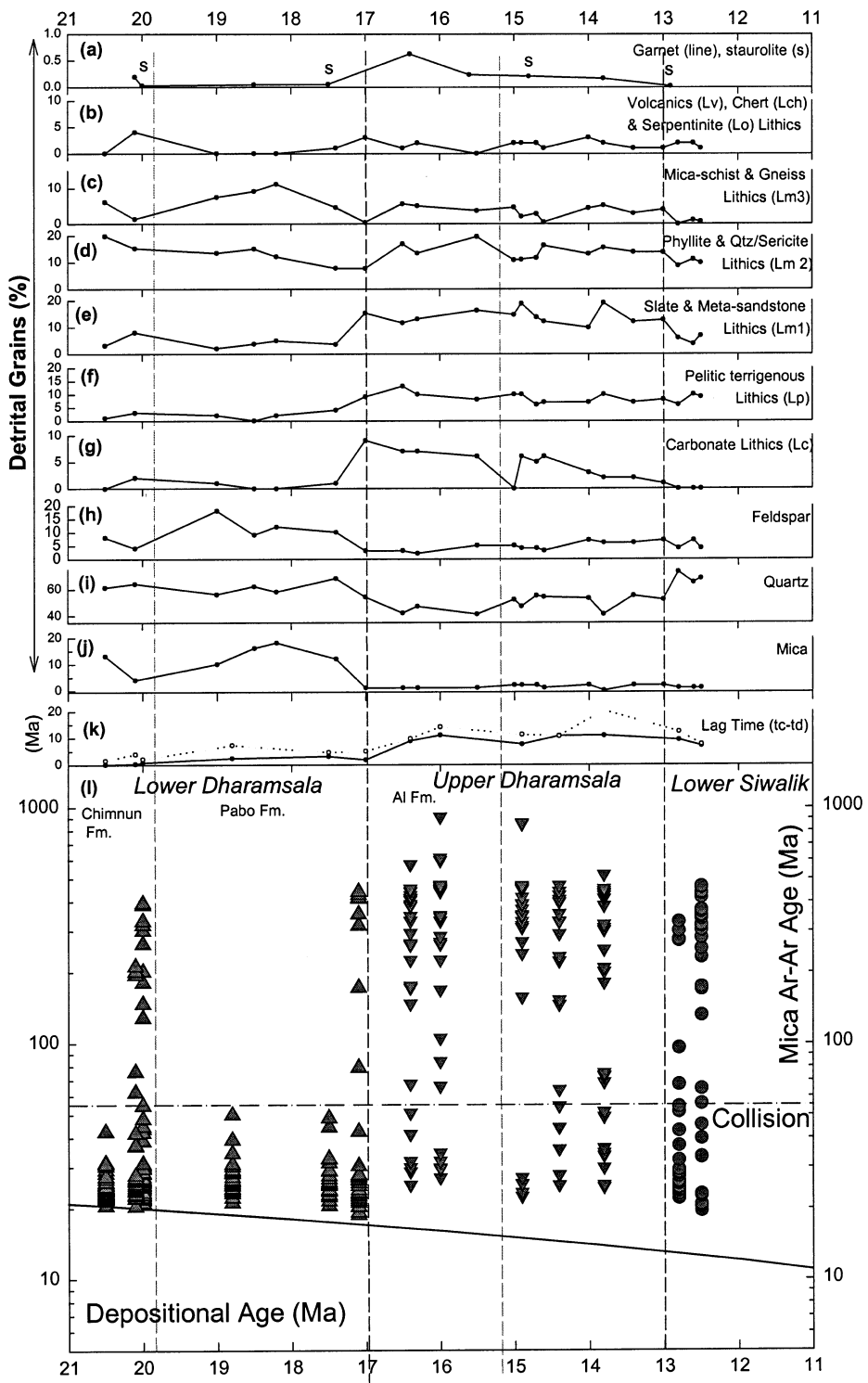
Fig. 4. Detrital composition and mica ages vs. time. Petrographic indexes plotted as percent detrital component (a–j) and single-grain detrital mica age data (k and l) are plotted against depositional age for the Dharamsala and Lower Siwalik sandstones. Dashed lines show the boundaries between formations. (a–i) Note a sharp decrease in detrital micas (j) and feldspars (h), with a corresponding increase in carbonate (g) to pelitic sedimentary grains (f), at the boundary between the Lower and Upper Dharamsala. Metasedimentary lithics are invariably abundant (c–e) with garnet and staurolite heavy minerals present (a). Detritus potentially derived from the suture zone is negligible (b). (k) The lag time, which is the difference between the youngest mica cooling age (t_c) and depositional age (t_d), is plotted against depositional age (solid line). Also shown is the modal mica lag time (dashed line). Note that the lag time is within 1–2 Ma for the Lower Dharamsala and increases to 7–8 Ma for the Upper Dharamsala and Lower Siwalik. (l) Single-grain mica ages (log scale) are plotted against time (linear scale). The dash-dot line represents the time of collision at ∼55 Ma and marks the division between 'Himalayan' (<55 Ma) and 'pre-Himalayan' (>55 Ma) mica ages. The 1:1 line (solid) where mineral age = depositional age is shown, mineral ages should lie above this line. Note the sharp decrease in Himalayan ages with an increase in pre-Himalayan ages at the boundary between the Lower and Upper Dharamsala.

←

dummy fuel element facility at the 1 MW TRIGA, Oregon State University. Three disks were irradiated for 12 h in the pool-side, Cd-lined RODEO facility at the 45 MW EU Commission HIFAR reactor, Petten, The Netherlands.

The irradiation flux parameter, *J*, was monitored with either the USGS standard sanidine from the Taylor Creek rhyolite (TCR-2a) at 27.92 Ma or the Fish Canyon tuff sanidine (FC-1) at 27.61 Ma loaded in eight wells located in an outer ring and in the centre well of each Cu disk. During the course of this study we discovered a ∼1.2% flux gradient between the outer and inner monitors, which may be attributed to self-shielding by the Cu disks. An average *J*, equal to 99.5% of the average of the outer ring monitors for each disk, was used. I.e. no attempt was made to correct each individual grain for the lower neutron flux toward the centre of the pan, introducing <0.5% error in the apparent age of each mica grain.

Irradiated Cu disks were loaded directly into the UHV vacuum line and baked at ∼150°C for 12–24 h. Single grains were fused or incrementally heated with a 20 or 25 W continuous CO_2 laser following Richards et al. [27]. Individual $^{40}Ar/^{39}Ar$ age and error calculations follow Dalrymple et al. [28]. Results are shown in Tables 1–3, in the **Background Data Set**[1], and Figs. 3–5; errors are quoted at the 2σ level of analytical precision. Plateau ages were calculated by weighting individual plateau steps by the inverse of the variance and corrected for excess scatter about

the mean when the *F* ratio statistic MSWD was greater than 1.

3.2. Bulk detrital composition studies

Three hundred points were counted on the 250–125 μm fraction of 21 selected fine-grained sandstones (Table 4, in the **Background Data Set**[1], Figs. 4,6 and 7) by the Gazzi–Dickinson method [29,30]. Detrital mineral and rock classification followed Najman and Garzanti [22] with metasedimentary clasts classified according to both composition (metapelites vs. metafelsites) and metamorphic grade (L_1 = slate and metasandstone, L_2 = phyllite, L_3 = mica-schist and gneiss). Two hundred and fifty transparent heavy minerals from the 63 to 250 μm size fraction of nine samples were counted on grain mounts (Table 5, in the **Background Data Set**[1], Fig. 6). Sample treatment followed [31]. Chemical compositions of significant minerals (tourmaline, staurolite, chloritoid) were analysed with an EDS microprobe at the Milano University.

3.3. Whole-rock Sr–Nd analyses

Rb–Sr and Sm–Nd isotope ratios were analysed on four samples of mudstone to siltstone (Table 6, in the **Background Data Set**[1]). Carbonate was removed by leaching with 1 M glacial acetic acid overnight. Comparison of leach and non-leached residues in one sample indicates that the carbonate contained a minor fraction of the Nd, but that leach and residue $^{87}Sr/^{86}Sr$ ratios differ (Fig. 8). Dissolution and analytical methods follow Ahmad et al. [32] except that the whole sample was

---

[1] http://www.elsevier.com/locate/epsl

spiked with a mixed ^{150}Nd–^{149}Sm spike and ^{143}Nd/^{144}Nd ratios measured on the spiked fraction. Sr blanks were less than 80 pg, a Sm blank contained 313 pg and a Nd blank 48 pg. Four analyses of the internal JM Nd standard gave ^{143}Nd/^{144}Nd = 0.511120 ± 14 (2σ) and ^{145}Nd/^{144}Nd = 0.348400 ± 10 over the period of the analyses. 18 analyses of NBS987 gave ^{87}Sr/^{86}Sr = 0.710257 ± 17 (2σ).

4. Results

4.1. ^{40}Ar–^{39}Ar detrital white mica analyses

Most detrital mica ages are determined by total fusion of individual grains which does not reveal the extent to which grains may have suffered partial loss of Ar. Incremental-heating experiments were therefore performed to test the degree of alteration (Fig. 3). Five micas younger than 40 Ma all yielded plateau ages concordant within 95% confidence intervals, i.e. MSWD < 2.5 (Fig. 3a). Single-grain ages from this age group can be interpreted as geologically meaningful. Incremental-heating results from micas older than 40 Ma show discordance. The alteration and Ar loss of these older grains precludes accurate determination of geologically meaningful cooling or crystallisation ages.

All the single-grain mica ages are plotted against depositional age (Fig. 4l), petrographic indexes (Fig. 4a–j) and lag time (Fig. 4k). There is a strong correlation between mica abundance and the age distribution of the micas. Fig. 5 shows histograms of the < 60 Ma Himalayan ages.

The sandstones of the Lower Dharamsala (*n* = 6) are micaceous (up to 14% of detrital grains), and 80 to 100% of the detrital grains have ages < 60 Ma with only occasional older ages (Fig. 4). Between 70 and 95% of the ages lie between 30 and 20 Ma, with modal values of 22–24 Ma (Fig. 5). The base of the section has detrital mica whose cooling ages differ from the stratigraphic age by less than 1 Ma (Fig. 4k). Towards the top of the Lower Dharamsala the lag time is ∼2–3 Ma (Fig. 4k). The strongly

skewed age distributions with the mode close to the minimum age and a tail towards maximum ages is expected from a terrain subject to variable exhumation rates, with maximum erosion (and thus detritus) from areas experiencing maximum exhumation (Fig. 5).
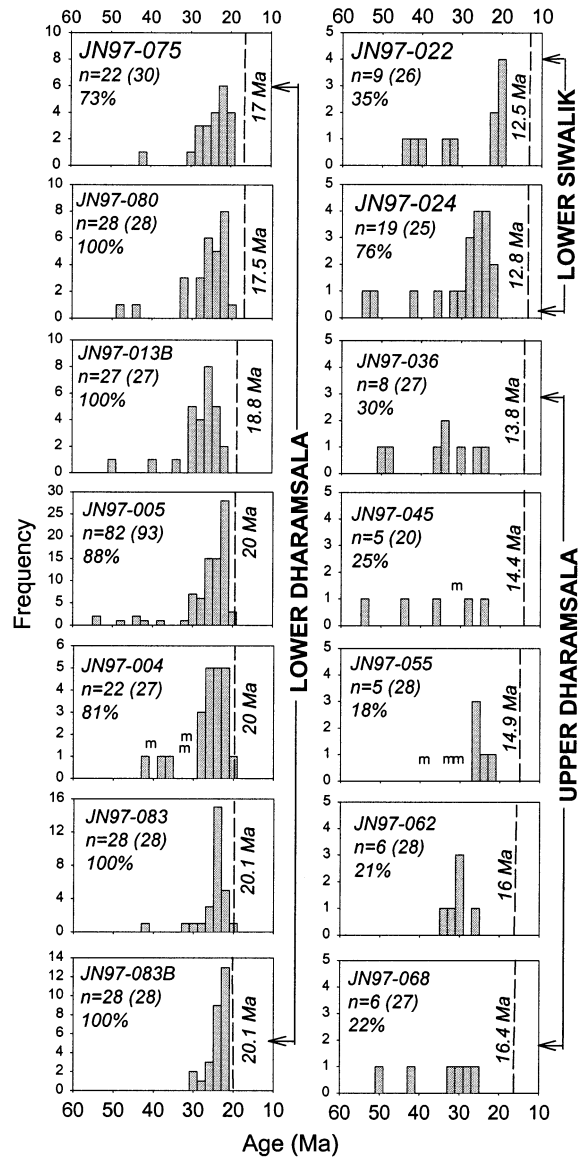

Fig. 5. Histograms of detrital white mica ages. The age of deposition is shown on the right (dashed line). Number of analysis (*n*) younger than 60 Ma are given out of the total grains analysed (), and as a percentage. Detrital monazite U–Th–Pb ages (M) from these sediments are also shown [6].

The Upper Dharamsala sandstones ($n = 5$) with ~1.5% modal mica are much less micaceous than the Lower Dharamsalas. Between 70 and 82% of these mica ages are >60 Ma reflecting thermal histories prior to the Indo–Asian collision. Most of the ages lie between 50 and 500 Ma but there are rare 800–950 Ma grains (Fig. 4l). Of the Himalayan aged grains (Fig. 5) the youngest (22–26

Ma) are slightly older than those in the Lower Dharamsalas and, therefore, the lag time increases to between 7 and 10 Ma (Figs. 4k and 5).

The sandstones at the base of the Lower Siwaliks ($n = 2$) have low abundances of detrital white mica (<1%). Ar–Ar ages range between 20 and 500 Ma (Figs. 4 and 5). The youngest mica ages (22 and 20 Ma) and modes of the <60 Ma micas
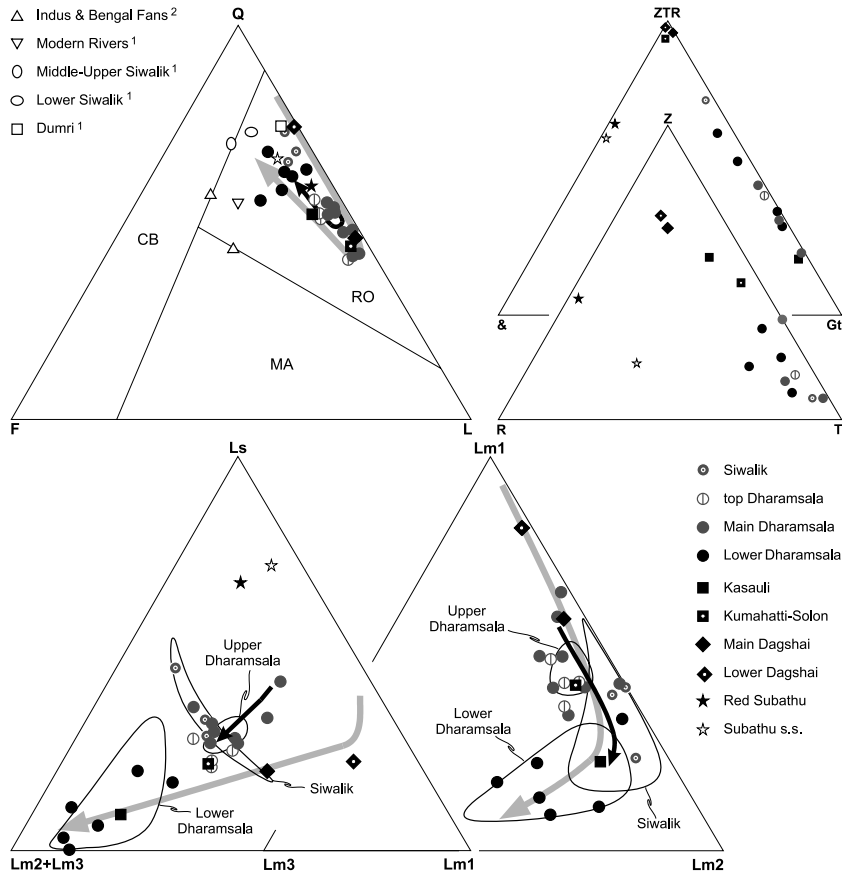

Fig. 6. Detrital composition plots. The composition of the Dharamsala sandstones reveal a major tectonic event at 17 Ma when progressive increase in grade of metamorphic detritus through time (grey arrows), well displayed from the Dagshai to Kasauli units (black squares and diamonds, data after Najman and Garzanti, [22]) and continued in the Lower Dharamsala sandstones (black circles) was abruptly reversed. Black arrows indicate the subsequent, less pronounced, renewed unroofing recorded in the Upper Dharamsala and Siwalik sandstones (grey circles). (QFL plot) The Himalayan foreland basin to remnant ocean sandstones all plot within the 'recycled orogen' (RO) provenance field ([41]; CB = continental block; MA = magmatic arc; the L pole includes carbonate and chert lithics). [1]Data after DeCelles et al. [42,43]; [2]Data after Ingersoll and Suczek [44] and [45]. (Ls–Lm1–Lm2 and Lm1–Lm2–Lm3 plots) Lithic grains in the Dharamsala to Siwalik Formations are mostly sedimentary (Ls) and metasedimentary (Lm) clasts derived from the Himalayan orogen. Means with 90% confidence regions calculated after Weltje [46]. (ZTR–Gt–& and ZTR Plots) Garnet (Gt) from medium grade Tertiary metamorphic rocks becomes dominant in the Kasauli and Dharamsala Formations. Ultrastable mineral grains (ZTR) are mostly rutile (R) in the Subathu Formation, zircon (Z) in the Dagshai and Kasauli Formations, and tourmaline (T) in the Dharamsala and Siwalik Formations. & = other minerals, including Cr-spinel in the Subathu Formation and staurolite in the Dharamsala and Siwalik Formations.

(24 and 26 Ma) give lag times of 7–9 Ma, similar to the Upper Dharamsala.

4.2. Petrography and dense minerals

The Lower Dharamsala sandstones ($n = 8$, average Q 62 F 10 L 28) contain abundant low- to medium grade metasedimentary clasts (Fig. 6) as well as metamorphic minerals including muscovite and biotite (4–18% of framework grains), abundant garnet (33–68% of heavy transparent minerals), tourmaline, zircon and rutile. Minor staurolite ($\leq$1%), chloritoid, epidote, chrome spinel, sphene, brookite and apatite are also found. Sedimentary and volcanic detritus including sandstone, sparite, chert and felsitic grains form a minor component (Fig. 6). Heavy mineral suites represent only 0.1–0.3% of the fine to very fine sand fraction. The sources of the Lower Dharamsala appear to be predominantly from low to medium grade (garnet–staurolite) mica-schists with only a minor component from little metamor-
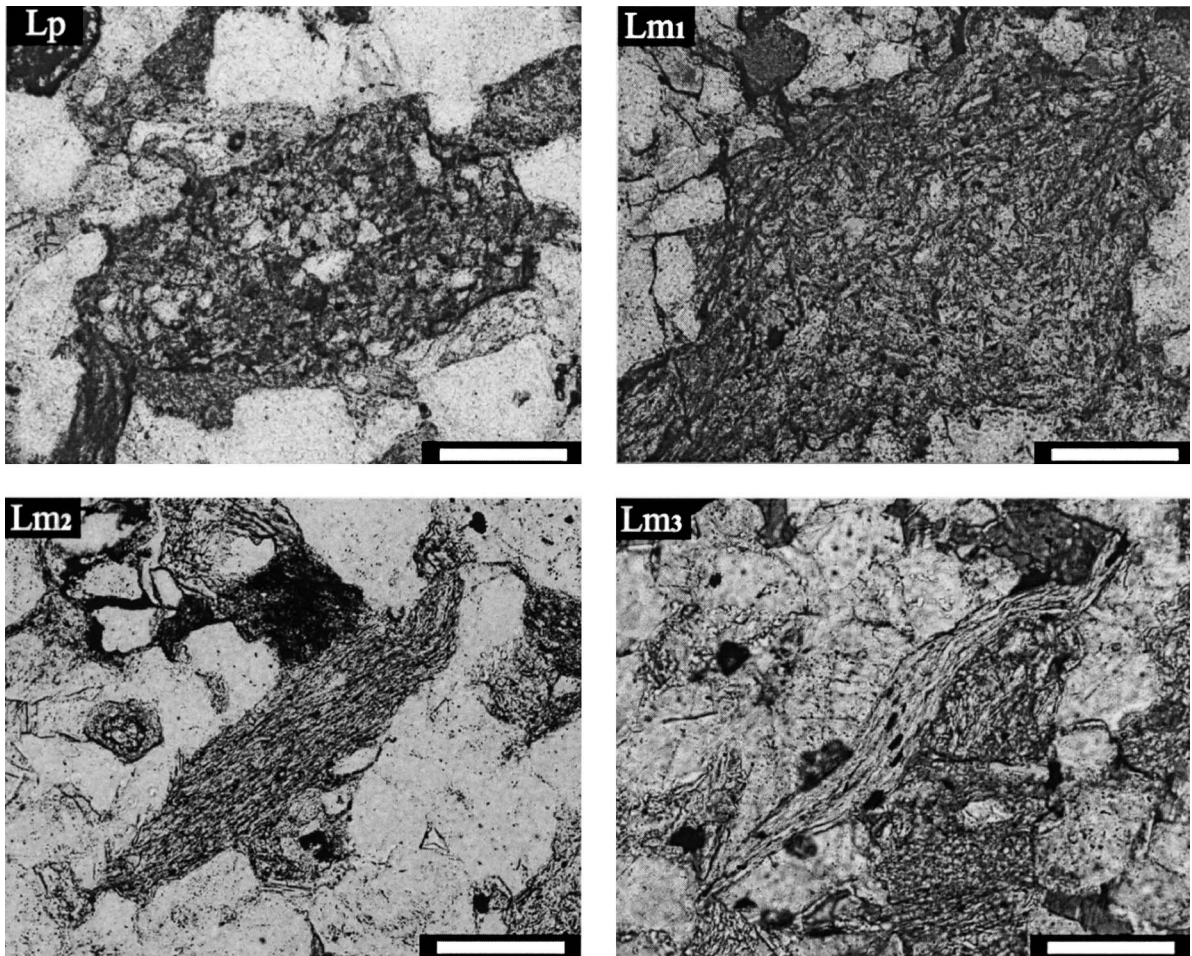

Fig. 7. Photomicrographs of lithic fragments. Classification of pelitic to metapelitic lithic grains (extended from Dorsey, [47]). Increasing degree of phyllosilicate crystallisation and progressive development of foliation provides precious information on metamorphic grade of Himalayan source rocks. Lp = siltstone lithic grain with unorientated clastic texture; Lm1 = slate lithic grain displaying tiny sericite and weak rough cleavage; Lm2 = phyllite lithic grain displaying sericite lamellae and strong cleavage; Lm3 = schist lithic grain displaying micaceous lamellae and schistocity.

phosed sedimentary and volcanic sources. This accords with the high proportion of very young micas indicating very rapid erosion of an active metamorphic source.

The Upper Dharamsala sandstones ($n = 10$, average Q 49 F 5 L 46) are dominated by sedimentary rock fragments (siltstone, micaceous sandstones, sparite and dolomite, and minor chert) and very low-to low grade metamorphic rock fragments (slate, phyllite, quartz–sericite and quartz–mica assemblages). Dolostone grains reach up to one third of total extrabasinal carbonate detritus (Fig. 6). Detrital micas are minor (1.5% of detrital grains). This abrupt change in provenance to predominantly sedimentary or very low grade sources and the reduction in the mica component is consistent with the Ar–Ar age data and the increase in lag times from ∼2 Ma to ∼10 Ma. However the micas and transparent heavy mineral suites dominated by garnet (locally reaching 4% of all detrital grains) with staurolite (≤1%), rare chloritoid and spinel indicate continued erosion of the medium grade metamorphic source. Significant recycling of Lower Dharamsala sediments is precluded by the lack of very young micas (<22 Ma) prominent in the Lower Dharamsala. The much higher proportion of heavy minerals (0.3–0.8% of the fine to very fine sand fraction) than in the Lower Dharamsala might reflect less selective leaching of less stable grains. A slight increase of feldspar in the upper part of the member (Fig. 6) hints at gradual unroofing of deeper-seated crystalline rocks.

The base of the Siwalik Group ($n = 3$, average Q 69 F 5 L 26) contains more quartz at the expense of metamorphic lithics, and carbonate rock fragments disappear. Metamorphic detritus largely consists of phyllite lithics (Fig. 6) and micas are few. Transparent heavy minerals dominated by tourmaline with garnet, zircon, rutile, staurolite, chloritoid and brookite indicate continued erosion of medium grade metamorphic sources. Dense minerals represent 0.1% of the fine to very fine sand fraction. We interpret the increased proportion of stable minerals as a consequence of enhanced chemical weathering which removed less stable grains either during diagenesis or prior to deposition.

4.3. Whole-rock isotopic compositions

Fig. 8 illustrates the Sr–Nd isotopic composition of four samples spanning the Dharamsala and basal Siwalik Groups compared to the fields of Himalayan source units [32], the Bengal fan and along strike foreland basin deposits [23,33]. $^{87}Sr/^{86}Sr$ ratios of 0.775 on the unleached and 0.785 on the leached fraction of Upper Dharamsala sample JN97-044 show that leaching removes a less radiogenic component whereas $^{143}Nd/^{144}Nd$ ratios are identical (Table 6, in the **Background Data Set**[1]). However both the unleached and residual leached $^{87}Sr/^{86}Sr$ ratios lie within the field of the HHCS as do the Sr isotopic ratios and all the measured Nd isotopic compositions of the other three samples. These results are consistent with the HHCS-dominated provenance inferred from Sr–Nd isotopic compositions of the older Dagshai and contemporaneous Kausuli Formations [23] and the results from the 17 to 0 Ma Bengal Fan [33]. The change in detrital petrography from a dominance of medium grade pelitic rocks to sedimentary and low grade rocks at 17 Ma cannot reflect uplift and erosion of the Lesser Himalayas but erosion from different structural levels of the High Himalayan Slab.
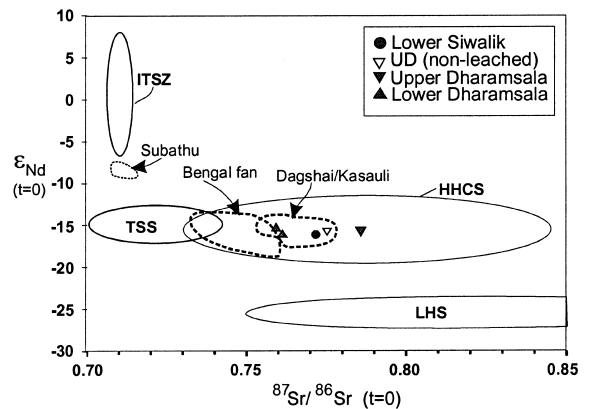

Fig. 8. Nd–Sr isotopic data from foredeep samples compared with Himalayan tectonic units and other Himalayan sedimentary basins (data compiled from Najman et al. [23] and references therein) on Nd–Sr isotopic diagram. The fields show that the Himalayan units have very different Sm–Nd and Rb–Sr isotopic systematics. Ellipses illustrate 1σ distributions of fields but with $^{87}Sr/^{86}Sr$ ratios >2 excluded from average LHS. UD = Upper Dharamsala.

5. Discussion

5.1. Provenance and exhumation

The combined results establish that the source of the sediments deposited during the Lower Dharamsala (∼20–17 Ma) included medium (garnet–staurolite) grade, micaceous, metamorphic rocks that cooled through mica blocking temperatures between 10 and 1 Myr prior to deposition, and which have isotopic compositions identical to the present day HHCS. We interpret the sediments to be primarily sourced from metamorphic rocks of the High Himalayan Slab in the footwall of the STDS. Minor chrome spinel, rutile and trace apatite, which decrease up-section, may have been derived from ophiolites in the Indus suture zone.

The cooling ages of between ∼30 and 20 Ma with skewed distributions towards young ages (Fig. 5) and lag times of 1–3 Ma (Fig. 4k) are compelling evidence for comparably rapid exhumation of their source region prior to 17 Ma. Simple thermal modelling allowing for advection modification of the geotherm demonstrates that the observed distribution of ages can be simulated with high rates of exhumation up to 5 mm/yr prior to deposition of the Lower Dharamsala Member, followed by exhumation rates of 1 mm/a from 20 Ma [26]. This is consistent with exposed HHCS rocks which were buried between >35 to <27 Ma [16] and then exhumed rapidly, contemporaneous with melting, extensional faulting on the STDS and thrusting on the MCT between ∼23 and 19 Ma [14].

The sediment sources and detrital mica ages change abruptly at the transition between the Lower Dharamsala and the Upper Dharamsala Members. The dominant source material changes from low to medium grade metamorphic rocks to sedimentary and very low grade metasedimentary source rocks indicating erosion of different structural levels of the orogenic wedge. The detrital micas change from distributions of predominantly Himalayan ages to predominantly pre-Himalayan ages up to 950 Ma. The Sr–Nd isotopic values do not vary significantly. The increase in carbonate

and pelitic rock fragments suggest the erosion of carbonates and shales.

We suggest that the source area for the Upper Dharamsala Member was the Chamba Nappe or an equivalent, which is exposed north of the Kangra basin and south of and structurally above the high grade HHCS (Fig. 1). This source would account for both low grade detritus from the Haimantas, and sedimentary detritus from the overlying Palaeozoic to Mesozoic Tethyan sediments. The Haimantas, regarded as the protolith of part of the HHCS [14] would, by implication, have the same isotopic composition. Ar loss in older grains precludes accurate provenance analysis, however, the >60–600 Ma mica ages may be a result of several thermal and tectonic events including the Late Cambrian to Early Ordovician Pan African orogenesis, Neo-Tethyan rifting during the Permo–Carboniferous, and an Early Cretaceous thermal event which affected the Indian plate rocks [8,34].

Continued erosion of the HHCS is indicated from the Upper Dharamsala sandstones and modelling of the detrital mica lag times suggests that after 17 Ma erosion rates of the HHCS were <1 mm/yr [26]. Petrographic results from the Upper Dharamsala Member suggests deepening of erosion levels (Fig. 6). The difference between the maximum staurolite–garnet grade source for the Dharamsala Group and the present day kyanite and sillimanite–migmatite grade of much of the exposed HHCS in NW India is consistent with limited (10–15 km) exhumation of the HHCS between 17 Ma and the present day [17].

A succession of ∼400 m of mudstones and thin sandstones, interpreted as overbank fines with crevasse splays or sheet flood deposits, is found at the transition between the Lower and Upper Dharamsala (Fig. 2). This contrasts with the thick multistory sandstone bodies, interpreted as channel deposits of large rivers, characteristic of both the Lower Dharamsala and the Upper Dharamsala overlying the finer grained transition zone. The finer grained interval may represent a period where the major river channel was located distally to this part of the basin. A shift in the location of major river channels in an active foreland setting

is expected following structural reorganisation within the orogenic wedge, which is likely to affect the river capture, subsidence, and uplift rates. A lack of convincing palaeocurrent information from the sediments and their distal nature precludes a more detailed interpretation of the fluvial response to the tectonics.

It is difficult to compare Upper Dharamsala sediments with the basal Siwalik sediments because of the increase in mineralogic stability in the latter which may be related to either superficial leaching or climate change. An abrupt increase in the tourmaline/garnet ratio coupled with much reduced heavy mineral concentrations in the basal Siwaliks suggest wider exposure of pre-Himalayan very low grade successions. A significant contribution from the LHS is precluded by the mica ages and Sr–Nd isotopic compositions.

5.3. Structural evolution of the hinterland

A simple interpretation of the dramatic shift in sediment provenance to predominantly sedimentary and low grade HHCS sources for the Upper Dharamsala and basal Siwalik Formations is that thrusting propagated southwards from the MCT to exhume the much less deeply eroded upper parts of the nappe pile. The southward transfer of thrusting would have terminated extension at the top of the HHCS sheet and drastically reduced thrust-related uplift of the rest of the metamorphic unit. However this simple interpretation is inconsistent with the present geology of the North West Indian Himalayas where the Chamba Nappe, low grade and sedimentary cover to the HHCS, tectonically overlies the metamorphic rocks on a SW dipping shear zone. An alternative model suggests that the apex of erosion, by 20 Ma, was from the upper structural parts of the HHCS (i.e. the footwall of the STDS rather than hanging wall of the MCT). This is consistent with the model of Grujic et al. [3] whereby ductile southward extrusion of the HHCS was modelled as channel flow. In this model the largest finite displacement is to be expected in the upper part of the channel. It is also consistent with models that couple deformation to surface erosion [2] and

imply that surficial processes exert a control on the geometry and location of exhumation. From 20–17 Ma channel flow and extrusion is likely to have ceased and propagation of thrusting down into the footwall of the MCT [35] resulted in the uplift and erosion of outlying low grade areas of the Chamba Nappe. This thrust may have been the MCT/Panjal Thrust or the Proto-MBT. This model is consistent with outcrop patterns and structural data from the HHCS cf. [36,12].

Interpretations of the tectonic setting during the Miocene from present outcrop patterns must be treated with caution, however, as convergence rates of $\sim 10 \pm 2$ mm/yr [37] imply ~ 170 km of shortening since 17 Ma.

5.4. Comparisons to other detrital studies

The Dharamsala and Siwalik sediments (20.5–12.5 Ma) studied here show both important similarities and differences to provenance and detrital mica age studies on Siwalik sediments deposited between 10.8 and ~ 2 Ma in Nepal [38] and Bengal Fan sediments between 17 and 0 Ma [33,39]. The Sr–Nd isotopic composition of the Bengal Fan sediments indicate their derivation predominantly from HHCS-like sources as for the Dharamsala sediments. Detrital muscovite and K-feldspar Ar–Ar ages from the Bengal Fan indicate very rapid exhumation of their sources post 17 Ma with lag times within error of zero, although the small population of both feldspar and muscovite ages with negative lag times is problematic. Likewise detrital K-feldspar Ar–Ar ages from the 10.8 to 2 Ma Siwalik molasse in Nepal have upper 2σ error bounds on lag times of 2–3 Ma. By contrast, although the lower Dharamsala sediments show small lag times of 2–3 Ma between 20.5 and 17 Ma, the lag times increase to 7–10 Ma in the Upper Dharamsala and basal Siwalik sediments. As the Bengal Fan receives sediment from two thirds of the Himalayan orogen, the locations of rapid exhumation are not constrained. This study shows that in the area of NW India sampled by the Dharamsala and basal Siwalik Formations in the Kangra basin, the detrital mineral ages match the mineral age patterns in the exposed rocks. Perhaps elsewhere continued mi-

gration or reactivation of the MCT has progressively exhumed younger metamorphic rocks [40].

6. Summary

Sr–Nd isotopic compositions, detrital mineralogy and petrography and Ar–Ar ages of detrital minerals are used to determine the nature and exhumation history of the sources of the sub-Himalayan Dharamsala and basal Siwalik sediments deposited in the Kangra basin and dated by magnetostratigraphy at between 20.5 and 12.5 Ma. Sr–Nd isotopic compositions of the sediments indicate that the whole sequence was derived from sources isotopically equivalent to the HHCS or its low grade equivalents. Prior to 17 Ma the abundance of medium grade metamorphic detritus, detrital garnet and staurolite, muscovite with lag times of 1–3 Ma and detrital monazites with ages between 40 and 29 Ma [6], indicate very rapid exhumation of HHCS rocks with a tectonic history similar to those presently exposed in the NW Indian Himalaya. After 17 Ma, the source for the Dharamsala sediments changed to predominantly sediments and low grade rocks similar to those in the Chamba Nappe which tectonically overlies HHCS metamorphic rocks. Detrital garnet and staurolite and a smaller fraction of Himalayan muscovite with ages in the same range of ∼ 30 to 22 Ma as from the Lower Dharamsala, confirm that erosion of medium metamorphic grade HHCS continued, albeit at much slower rates. This change in provenance is interpreted to indicate a fundamental reorganisation of the orogenic wedge geometry in the NW Indian Himalayas at 17 Ma, with cessation of extension on the STDS and propagation of thrusting south from the MCT.

The marked decrease in exhumation rate inferred from the Dharamsala sediments in the Kangra basin contrasts with detrital K-feldspar ages from the 10.8 to 2 Ma Siwalik sub-Himalayan sediments from Nepal and detrital K-feldspar and muscovite ages from a 17 to 0 Ma section of the Bengal Fan which both exhibit very short lag times indicative of continued rapid exhumation in other parts of the Himalaya. This

demonstrates the value of more proximal and smaller-scale studies in elucidating the variability and timing of processes in large orogenic belts.

References

[1] P.C. England, S.W. Richardson, The influence of erosion upon the mineral facies of rocks from different metamorphic environments, J. Geol. Soc. Lond. 134 (1977) 201–213.

[2] C. Beaumont, R.A. Jamieson, M.H. Nguyen, B. Lee, Himalayan tectonics explained by extrusion of a low-viscosity crustal channel coupled to focused surface denudation, Nature 414 (2001) 738–742.

[3] D. Grujic, M. Casey, C. Davidson, L.S. Hollister, R. Kundig, T. Pavlis, S. Schmid, Ductile extrusion of the Higher Himalayan Crystalline in Bhutan evidence from quartz microfabrics, Tectonophysics 260 (1996) 21–43.

[4] P.K. Zeitler, A.S. Meltzer, P.O. Koons, D. Craw, B. Hallet, C.P. Chamberlain, W.S.F. Kidd, S.K. Park, L. Seeber, M. Bishop, J. Schroder, Erosion, Himalayan geodynamics, and the geomorphology of metamorphism, GSA Today 11 (2001) 4–9.

[5] A.I. Chemenda, J.P. Burg, M. Mattauer, Evolutionary model of the Himalaya–Tibet system: geopoem based on modelling, geological and geophysical data, Earth Planet. Sci. Lett. 174 (2000) 397–409.

[6] N.M. White, R.R. Parrish, M.J. Bickle, Y.M.R. Najman, D. Burbank, A. Maithani, Metamorphism and exhumation of the NW Himalaya constrained by U–Th–Pb analysis of detrital monazite grains from early foreland basin sediments, J. Geol. Soc. Lond. 158 (2001) 625–635.

[7] D.B. Rowley, Age of initiation of collision between India and Asia: A review of stratigraphic data, Earth Planet. Sci. Lett. 145 (1996) 1–13.

[8] M. Gaetani, E. Garzanti, Multicyclic history of the Northern India Continental margin (northwestern Himalaya), Am. Assoc. Pet. Geol. Bull. 75 (1991) 1427–1446.

[9] E. Garzanti, T. Van Haver, The Indus clastics: forearc basin sedimentation in the Ladakh Himalaya (India), Sediment. Geol. 59 (1988) 237–249.

[10] M.P. Searle, D.J. Waters, D.C. Rex, R.N. Wilson, Pressure, temperature and time constraints on Himalayan metamorphism from eastern Kashmir and western Zanskar, J. Geol. Soc. Lond. 149 (1992) 753–773.

[11] K.S. Valdiya, S.B. Bhatia, Stratigraphy and Correlations of Lesser Himalayan Formations, Hindustan Publishing Corporation, India, 1980, 330 pp.

[12] V.C. Thakur, Structure of the Chamba nappe and position of the Main Central Thrust in Kashmir Himalaya, J. Asian Earth Sci. 16 (1998) 269–282.

[13] U. Pognante, D. Castelli, P. Benna, G. Genivese, F. Oberli, M. Meier, S. Tonarini, The crystalline units of the High Himalayas in the Lahaul–Zanskar region (northwest India) metamorphic – tectonic history and geochronology of the collided and imbricated Indian plate, Geol. Mag. 127 (1990) 101–116.

[14] J.D. Walker, M.W. Martin, S.A. Bowring, M.P. Searle, D.J. Waters, K.V. Hodges, Metamorphism, melting, and extension: Age constraints from the High Himalayan slab of southeast Zanskar and northwest Lahaul, J. Geol. 107 (1999) 473–495.

[15] P.M. Powers, R.J. Lillie, R.S. Yeats, Structure and shortening of the Kangra and Dehra Dun reentrants, Sub-Himalaya, India, GSA Bull. 110 (1998) 1010–1027.

[16] D. Vance, N. Harris, Timing of prograde metamorphism in the Zanskar Himalaya, Geology 27 (1999) 395–398.

[17] M.P. Searle, D.J. Waters, M.W. Dransfield, B.J. Stephenson, C.B. Walker, J.D. Walker, D.C. Rex, Thermal and mechanical models for the structural and metamorphic evolution of the Zanskar High Himalaya, in: C. Mac Niocaill, P.D. Ryan, (Eds.), Continental Tectonics, Geol. Soc. Spec. Publ., London, 1999, pp. 139–156.

[18] P.J. Dezes, J.C. Vannay, A. Steck, F. Bussy, M. Cosca, Synorogenic extension: Quantitative constraints on the age and displacement of the Zanskar shear zone (northwest Himalaya), GSA Bull. 111 (1999) 364–374.

[19] K.V. Hodges, R.R. Parrish, M.P. Searle, Tectonic evolution of the central Annapurna Range, Nepalese Himalaya, Tectonics 15 (1996) 1264–1291.

[20] A.J. Meigs, D.W. Burbank, R.A. Beck, Middle-late Miocene (>10 Ma) formation of the Main Boundary Thrust in the western Himalaya, Geology 23 (1995) 423–426.

[21] P. Molnar, Structure and tectonics of the Himalaya: constraints and implications of geophysical data, Annu. Rev. Earth Planet. Sci. 12 (1984) 498–518.

[22] Y. Najman, E. Garzanti, Reconstructing early Himalayan tectonic evolution and palaeogeography from Tertiary foreland basin sediments, Northern India, Geol. Soc. Am. Bull. 112 (2000) 435–449.

[23] Y. Najman, M. Bickle, H. Chapman, Early Himalayan exhumation: Isotopic constraints from the Indian foreland basin, Terra Nova 12 (2000) 28–34.

[24] D.W. Burbank, R.A. Beck, T. Mulder, The Himalayan Foreland Basin, in: A. Yin, T.M. Harrison (Eds.), The Tectonic Evolution of Asia, 1996, pp. 149–188.

[25] V. Raiverman, B.T.V. Sheshavataram, On mode of deposition of Subathu and Dharamsala sediments in the Himalayan foothills in Punjab and Himachal Pradesh, Wadia Commemorative Volume, 1965, pp. 556–571.

[26] N.M. White, The Early to Middle Miocene Exhumation History of the High Himalayas, NW India, Ph.D. Thesis, Department of Earth Sciences Cambridge University, Cambridge, 2001, 195 pp.

[27] J.D. Richards, S.R. Noble, M.S. Pringle, A revised Late Eocene age for porphyry copper mineralisation in Esconda area, Northern Chile, Econ. Geol. 94 (1999) 1231–1248.

[28] G.B. Dalrymple, D.A. Clague, M.O. Garcia, S.W. Bright, Petrology and K–Ar ages of dredged samples from Laysan Island and Northhampton Bank Volcanos, Hawaiian Ridge, and evolution of the Hawaiian ridge, and evolution of the Hawaiian-Emperor chain-summary, Geol. Soc. Am. Bull. 92 (1981) 315–318.

[29] R.V. Ingersoll, T.F. Bullard, R.L. Ford, J.P. Grimm, J.D. Pickle, S.W. Sares, The effect of grain size on detrital modes: a test of the Gazzi-Dickenson point-counting method, J. Sediment. Petrol. 54 (1984) 103–116.

[30] G.G. Zuffa, Optical analysis of arenites: Influence of methodology on compositional results, in: G.G. Zuffa (Ed.), Provenance of arenites, NATO Advanced Study Institute, 1985, pp. 165–189.

[31] A. Parfenoff, C. Pomerol, J. Tourenq, Les Mineraux en grains: Methodes d'etude et determination, Masson, Paris, 1970, 576 pp.

[32] T. Ahmad, N. Harris, M. Bickle, H. Chapman, J. Bunbury, C. Prince, Isotopic constraints on the structural relationships between the Lesser Himalayan Series and the High Himalayan Crystalline Series, Garhwal Himalaya, Geol. Soc. Am. Bull. 112 (2000) 324–350.

[33] C. France-Lanord, L Derry, A. Michard, Evolution of the Himalaya since Miocene time: isotopic and sedimentological evidence from the Bengal Fan, in: P.J. Treloar, M.P. Searle (Eds.), Himalayan Tectonics, Geol. Soc. Spec. Publ., London, 1993, pp. 603–621.

[34] E. Garzanti, Stratigraphy and sedimentary history of Nepal Tethys Himalaya passive margin, J. Asian Earth Sci. 17 (1999) 805–827.

[35] B.J. Stephenson, M.P. Searle, D.J. Waters, D.C. Rex, Structure of the Main Central Thrust zone and extrusion of the High Himalayan deep crustal wedge, Kishtwar–Zanskar Himalaya, J. Geol. Soc. Lond. 158 (2001) 637–652.

[36] B.J. Stephenson, D.J. Waters, M.P. Searle, Inverted metamorphism and the Main Central Thrust: field relations and thermobaric constraints from the Kishtwar Window, NW Indian Himalaya, J. Metamorph. Geol. 18 (2000) 571–590.

[37] P. England, P. Molnar, Active deformation of Asia: from kinematics to dynamics, Science 278 (1997) 647–650.

[38] T.M. Harrison, P. Copeland, S.T. Hall, J. Quade, S. Burner, T.P. Ojha, W.S.F. Kidd, Isotopic preservation of Himalayan/Tibetan uplift, denudation, and climatic histories of two molasse deposits, J. Geol. 101 (1993) 157–175.

[39] P. Copeland, T.M. Harrison, Episodic rapid uplift in the Himalaya, Geology 18 (1990) 354–357.

[40] E.J. Catlos, T.M. Harrison, M.P. Searle, M.S. Hubbard, Evidence for Late Miocene reactivation of the Main Central Thrust: From Garhwal to the Nepali Himalaya, 14th Himalaya-Karakorum-Tibet Workshop, Kloster Ettal, Germany (abstr.), 1999.

[41] W.R. Dickenson, Interpreting provenance relations from detrital modes of sandstones, in: G.G. Zuffa (Ed.), Provenance of Arenites, D. Reidel, Boston, MA, 1985, pp. 331–361.

[42] P.G. DeCelles, G.E. Gehrels, J. Quade, T.P. Ojha, Eocene–Early Miocene foreland basin development and the history of Himalayan thrusting, western and central Nepal, Tectonics 17 (1998) 741–765.

[43] P.G. DeCelles, G.E. Gehrels, J. Quade, T.P. Ojha, P.A. Kapp, B.N. Upreti, Neogene foreland basin deposits, erosional unroofing, and the kinematic history of the Himalayan fold–thrust belt, western Nepal, Geol Soc. Am. Bull. 110 (1998) 2–21.

[44] R.V. Ingersol, C.A. Suczec, Petrology and provenance of Neogene sand from Nicobar and Bengal Fans, DSDP sites 211 and 218, J. Sediment. Petrol. 54 (1979) 1217–1228.

[45] C.A. Suczek, R.V. Ingersol, Petrography and provenance of Cenozoic sand from the Indus cone and the Arabian Basin, DSDP sites 221, 222, and 224, J. Sediment. Petrol. 55 (1985) 340–346.

[46] G.J. Weltje, Construction of predictive regions in ternary diagrams: Towards statistically rigorous provenance studies, Geology Department Internal Report, Utrecht University, Utrecht, 1998, 28 pp.

[47] R.J. Dorsey, Provenance evolution and unroofing history of a modern arc-continent collision Evidence from petrography of Plio-Pleistocene sandstones, eastern Taiwan, J. Sediment. Petrol. 58 (1988) 208–218.